

COMPUTATIONAL SIMULATION OF ACOUSTIC MODES IN ROCKET COMBUSTORS

C. L. Merkle, V. Sankaran and M. Ellis

Purdue University

West Lafayette IN

ABSTRACT

A combination of computational fluid dynamic analysis and analytical solutions is being used to characterize the dominant modes in liquid rocket engines in conjunction with laboratory experiments. The analytical solutions are based on simplified geometries and flow conditions and are used for careful validation of the numerical formulation. The validated computational model is then extended to realistic geometries and flow conditions to test the effects of various parameters on chamber modes, to guide and interpret companion laboratory experiments in simplified combustors, and to scale the measurements to engine operating conditions. In turn, the experiments are used to validate and improve the model. The present paper gives an overview of the numerical and analytical techniques along with comparisons illustrating the accuracy of the computations as a function of grid resolution. A representative parametric study of the effect of combustor mean flow Mach number and combustor aspect ratio on the chamber modes is then presented for both transverse and longitudinal modes. The results show that higher mean flow Mach numbers drive the modes to lower frequencies. Estimates of transverse wave mechanics in a high aspect ratio combustor are then contrasted with longitudinal modes in a long and narrow combustor to provide understanding of potential experimental simulations.

INTRODUCTION

Combustion instability has plagued many liquid rocket engine development programs. Its impact can range from minor 'rough' burning incidents to highly catastrophic events. The most dominant characteristic of combustion instability is its unpredictability. A given test program can proceed smoothly with no indication of difficulty and then suddenly encounter an instability incident. The incident may be triggered by a scale-up to a new combustor size, a small change in design, or even something as minor as a change in the fuel temperature. Unequivocal means for establishing that a given design will not encounter difficulty do not exist. It is perhaps even more difficult to demonstrate that the mechanisms that have previously caused an engine to encounter difficulty have been effectively mitigated. The ethereal nature of instability is perhaps best noted by indicating that for years the SSME engine flew with baffles in the chamber even though it now appears they were never needed.

The tendency toward instability is strongly affected by the injector element and the fuel. Historically hydrocarbon engines have proven to be much more susceptible to instability than hydrogen engines, however, the reason for this susceptibility must be considered carefully. Most hydrocarbon engines in the US have employed impinging injectors while cryogenic engines have typically used co-axial elements. Consequently it is important to ascertain whether the susceptibility to unstable combustion arose from the hydrocarbon fuel or the impinging element. Current preference for hydrocarbon engines is to move from impinging elements to swirling coax elements (often with recess) thereby placing our historical database in question. How applicable is the existing hydrocarbon/impinging element data base to these radically different injector types? Further, current interest in cryogenic engines raises the possibility of injecting liquid rather than gaseous hydrogen. This raises the corresponding question: Is hydrocarbon fuel more prone to instability than is hydrogen, or is the liquid phase more prone than gaseous fuels? Clearly, there are many important issues to be addressed in dealing with combustion instability.

The present paper describes the analytical portion of an on-going study on combustion instability that closely couples detailed modeling with laboratory-scale experiments. The goal is

to combine the recent dramatic advances in experimental diagnostics with the equally dramatic advances in computational capabilities to provide improved understanding of combustion instability. Emphases are on documenting combustor environments and developing improved modeling tools (modeling here covers both scale-model experiments and computation). The experimental components of the study are discussed elsewhere [1,2]. The focus of the paper is on assessing the effects of flowfield variables on the acoustic modes of chambers with emphasis on two possible experimental configurations, one designed to generate longitudinal disturbances and the other for transverse disturbances. The goals are to ascertain the response of the injector to forced disturbances of both types of waves as means of characterizing their suitability for stable combustion.

RESULTS AND DISCUSSION

Detailed computational simulations are very promising for studying combustion instability because they provide complete detail on mode shapes and amplitudes and allow complete nonlinear effects to be simulated. There are, however, two primary shortcomings of computational simulations. First, each simulation provides stability information at only one condition so that many hundreds of calculations are needed to map out a stability diagram. Second, the numerical simulations must be validated to assess their accuracy. While experimental results are crucial for validating steady state computations, they become less so for unsteady phenomena because it is so difficult to provide the massive quantities of data needed at the accuracy levels required to truly validate a code. For both of these reasons, we supplement our computational solutions by means of a linearized analytical model of the flow in a chamber. To keep the analysis simple, we use simple geometries and simple physics in the analytical model. The closed-form solutions then provide an effective overview of the topography of instability zones, while also providing very precise results against which the computations can be verified. After ascertaining that the numerical simulations are providing an accurate solution to the model that has been posed, experimental results are required to validate the quality of the model itself. In addition, the computational simulations allow us to build upon the basic framework set up by the analytical model to incorporate additional geometrical complexities, more complex physical submodels and effects of large amplitude waves and nonlinearities.

In the following subsections, we begin by summarizing the computational model and the analytical model. Following this we present a series of results showing the effects of mean flow Mach number on the amplitude of forced disturbances and the effect of different upstream boundary conditions.

COMPUTATIONAL MODEL

The computational solutions are obtained with our in-house GEMS (General Equation and Mesh Solver) code [2-5]. GEMS uses a dual time scheme for time-accurate results such as the present one. This formulation is chosen because it is not only more efficient, but can also be more accurate for a wide range of flow speeds. The formulation uses a generalized unstructured grid method with second-order-flux split upwinding for the convective terms and Galerkin's method for diffusive terms. Although the code has capability for complete reaction kinetics, the present results represent solutions of the inviscid Euler equations for a perfect gas with constant specific heats. The mean flow Mach numbers in the present results range from 0.05 to 0.5, with the lower Mach numbers being representative of the planned laboratory-scale experiments [1,2], while the higher Mach numbers are representative of full-scale rocket engine operating conditions. Analysis of unsteady computations shows that it is necessary to add preconditioning to the upwinded discretization used in the dual time to prevent the solution from being swamped by excess artificial dissipation at these very low Mach numbers [4,5]. For this reason, the present calculations were all carried out with preconditioning. The present solutions are formally second-order accurate in time and space.

ANALYTICAL MODEL

As indicated above a closed-form analytical solution is used to map the topography of the stability plane and discern the characteristics of the various mode shapes. In addition, these analytical solutions serve as the first validation step for the computational simulations. Analytical solutions allow comparison of complete mode shapes, amplitudes and phases, providing a highly effective check of the solutions. Because the primary purposes of the analytical solution are for understanding global effects and for validating detailed portions of the computations, closed-form solutions need only be obtained for simple geometries and need only incorporate simple physics. The computational solution can then be used to extend the analytical findings to more complex domains and more complicated physics. It is, however, necessary that the analytical solution be formulated for boundary conditions that are identical to those that will be used in the numerical simulations (to ensure that the boundary conditions are validated along with the global formulation) and that it be identical to the numerical solution in other aspects as well.

The closed-form solution is obtained from a frequency-domain analysis of the linearized Euler equations that gives the acoustic modes in a chamber that has inflow and outflow at the upstream and downstream boundaries. The left-most geometry in Fig. 1 shows a representative geometry for the analytical solution while the two on the right show geometries of interest for the computational simulations. In this figure, the flow goes from left to right, and the goal is to assess transverse disturbances in a chamber with mean flow. Using a constant area passage with a constant mean Mach number simplifies the analytical solution while still providing a global understanding of the unsteady flow characteristics. The remaining two plots in Fig. 1 show geometries that were computed with the numerical model to incorporate the effects of finite length nozzles with multiple exit ports to simulate a possible experimental configuration. Analytical solutions with long chambers that support longitudinal modes (Fig. 2) have also been computed as discussed below.

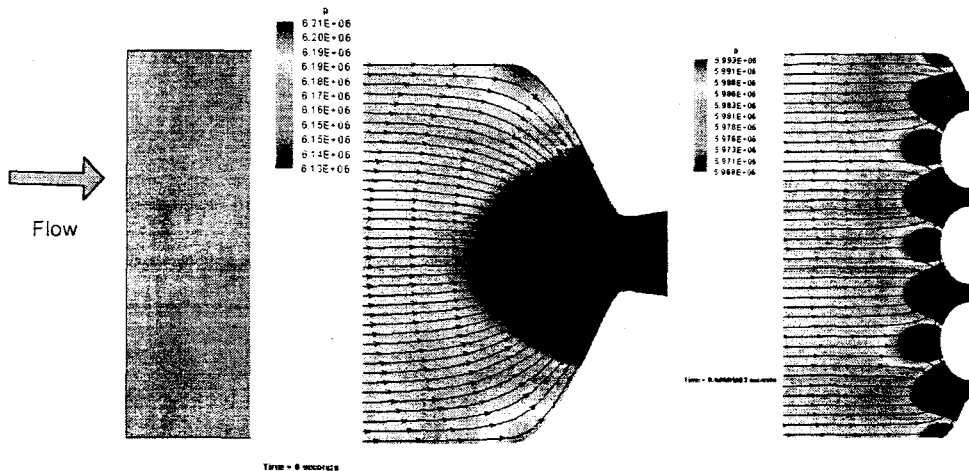


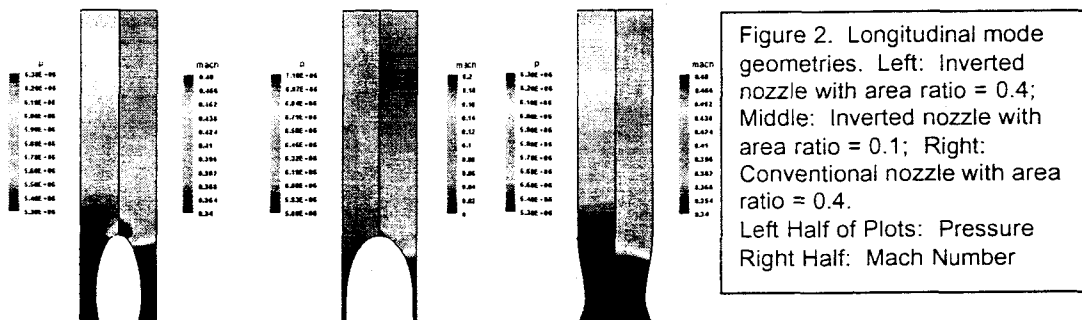
Figure 1. Geometry for analytical solution and computational validation (left) and multiple nozzle numerical simulations (center and right). Transverse mode analyses.

Perturbations in a constant-area duct with a uniform mean flow are easily solved analytically. For our formulation, we have specified boundary condition forcing at the upstream end or the downstream end. Boundary condition pairs at the upstream end are either the stagnation temperature and stagnation pressure or the mass flow and stagnation pressure. In both cases, the v -velocity component is set to zero. At the downstream boundary, the static pressure is specified. Boundary conditions at either end can be specified as constant or an arbitrary function of cross-stream distance and time (expressed as a Fourier series) to see the response to forcing. Results given below refer to both upstream and downstream forcing.

MEAN FLOW MACH NUMBER EFFECTS—LONGITUDINAL COMBUSTOR

As a first example we consider a chamber that is designed to support longitudinal oscillations [2] and driven by a pressure oscillation at the downstream end. The generic geometry, which is intended to represent a uni-element combustor, is shown in Fig. 2. The combustor has a diameter of two inches and a length of six inches followed by a two-inch nozzle. In the projected experiment [2] the combustor length would be variable, but here we characterize only a fixed tube length. Downstream forcing would be accomplished experimentally by a siren-like device. For the analytical solutions which are based on a constant area duct, we use a duct length of eight inches to replace the nozzle. Companion numerical simulations were also done for this same constant area geometry. The chamber conditions are specified as 65 atm and 3100 K, chosen to approximately match an RP-1/oxygen propellant combination. At these conditions the first longitudinal mode in the eight inch duct is approximately 3000 Hz.

As noted above, the analytical solutions were obtained in the frequency domain. For a given set of conditions, the frequency response was obtained by computing the pressure variation at the head end to a series of sinusoidally varying pressures at the downstream end. The results are then presented as the ratio of the peak pressure at the head end divided by the amplitude of the downstream forcing function. For these longitudinal mode studies, the pressure forcing at the downstream boundary was accomplished by pure mode oscillations with uniform pressures across the area (oscillation in time only). By contrast with the frequency domain results for the analytical solution, the numerical results were obtained by marching in time while forcing at a given frequency. The time-domain solutions required an initial transient period for the initial condition (uniform flow without perturbation) to die down. The stationary oscillations were then measured from temporal oscillations after this transient was completed. The results are again reported as the ratio of the amplitude of the head-end oscillation to the amplitude of the forcing function. The goals of this initial set of results are to compare the analytical solutions with the computational simulations with the dual goal of understanding the physics and assessing the accuracy of the computations. For this longitudinal oscillation both the numerical and the analytical solutions were one-dimensional in character. Nevertheless the numerical solutions were obtained with the axisymmetric code using a coarse grid in the radial direction.



As a parameter in this first set of solutions, we consider four different combustor mean flow Mach numbers, $M = 0.05, 0.1, 0.3$ and 0.5 . Typical mean flow Mach numbers in full-scale engines are typically around 0.3, whereas packaging constraints along with a desire for optical access drives uni-element combustors to substantially lower Mach numbers. One of the goals of this series of results is to document the role of the mean flow Mach number on the amplification characteristics of disturbances, while another is to identify scaling issues between uni-element full scale testing. In combination with the transverse mode simulations given below, the present longitudinal oscillations are intended as a calibration of the sensitivity of a given injector element to transverse disturbances.

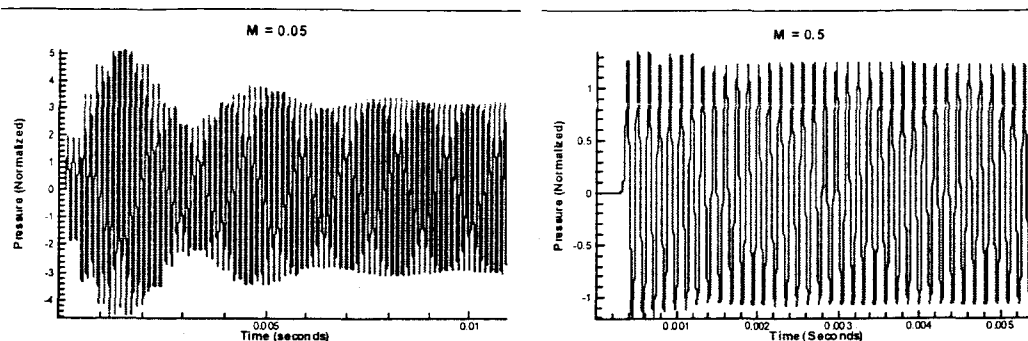


Figure 3. Time history of pressure at a point—numerical simulation. Left: $M = 0.05$, Right: $M = 0.5$.

As an initial indication of the effects of the mean flow Mach number on the solutions, we present in Fig. 3, the time-history of the pressure oscillations at one point in the computational domain for two different mean flow Mach numbers. The plot on the left of Fig. 3 corresponds to a Mach number of 0.05, while the plot on the right shows the pressure-time history for an $M = 0.5$ condition. The important trend to note is that the length of the transient is much longer at the lower Mach number condition where a stationary oscillation is not quite reached after 0.01 seconds. By contrast, the plot on the right shows that the oscillation has become stationary after approximately 0.0015 seconds. (Note that the time span of the plot on the left is twice that on the right.) The time to steady state is therefore approximately inversely proportional to the mean flow Mach number. The reason is that the flow in the combustor must be completely convected out the downstream boundary before the oscillation can become stable (despite the fact that the oscillation is small enough to be linear). Second, note that the amplitude of the plot on the left is approximately three times as large as that on the right (note scale change). This is a general observation that as the flow Mach number decreases, the magnitude of the pressure gain at the upstream end is increased. In addition the frequency is decreased substantially as noted below.

The effect of Mach number on both the amplitude and resonant frequency of the disturbance is more readily seen from the four plots in Fig. 4 which show the normalized pressure at the head end resulting from forcing at the downstream end for the four Mach numbers listed above. The plot at the upper left corresponds to a mean flow Mach number of 0.05, while that at the upper right is $M = 0.1$, the lower left is for $M = 0.3$ and the lower right for $M = 0.5$. These plots contain both computational and analytical results. The computational results are obtained from a sequence of numerical solutions like those shown in Fig. 3. The analytical results represent a standard frequency-domain analysis. A quick comparison of the numerical and analytical results in all four plots shows that the numerical results are in excellent agreement with the exact solutions. Additional detail on grid resolution is given later.

In addition to demonstrating the accuracy of the numerical results, the results in Fig. 4 also demonstrate the effect of mean flow Mach number on the pressure response. Both the pressure scale and the frequency scale are identical in all four plots so the relative magnitudes and frequencies can be obtained by visually comparing the heights of the frequency response. The pressure amplitude decreases continuously from $M = 0.05$ to $M = 0.5$ with a total reduction in amplitude of nearly an order of magnitude. This implies that an important scaling from uni-element tests to full scale combustors will occur through the Mach number. Since (as noted above) uni-element tests typically have lower mean flow Mach numbers than full-scale combustors, the pressure amplitudes obtained by downstream forcing will likely overestimate those seen in full scale combustors. This provides disturbance amplification that will be easier to measure in uni-element combustors and also implies that they will provide conservative scaling as compared to full-scale applications. The process is, however, complex and other factors will most certainly be present. We also note that there is a considerable downward shift in the

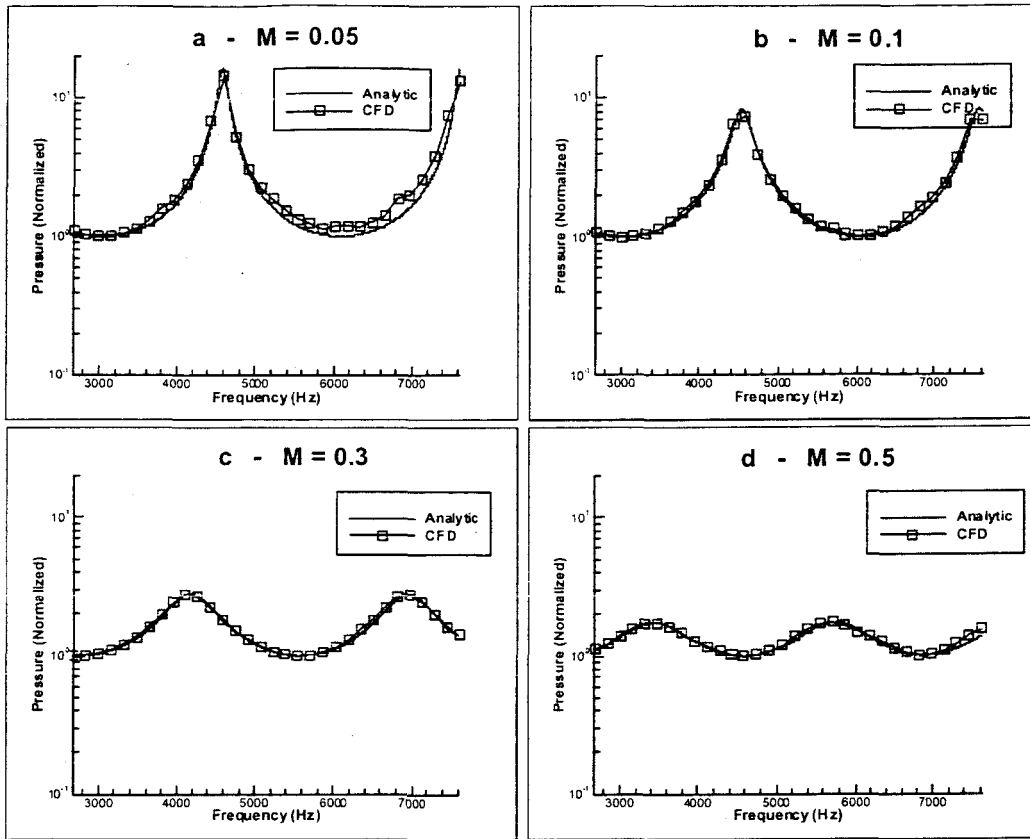


Figure 5. Frequency response of longitudinal chamber for four mean flow Mach numbers: 0.05, 0.1, 0.3, and 0.5, showing comparison between exact analytical solution and numerical simulations. Downstream forcing with upstream mass flux fixed.

frequency of both the first and second modes as the Mach number is increased. At a mean flow Mach number of 0.05, the first longitudinal mode is very close to the classical result for acoustic modes in a quiescent medium. As the Mach number is increased to 0.5, this first mode frequency is decreased by nearly 50%. Larger Mach numbers also increase the width of the 'resonant' peaks. This change in resonant-mode frequency with Mach number is the result of $u+c$ and $u-c$ effects. Finally, we note that the shape of the frequency response curves changes substantially as the Mach number is increased. At low Mach numbers, the response is sharply peaked and narrow akin to behavior observed in quiescent environments, but at higher Mach numbers, the peaks are much more rounded and gentle so the distinction between off-resonance and on-resonance is much smaller. Again, note that these observations are for longitudinal modes.

In terms of the comparison between numerical and analytical results, we note that the numerical comparison for the lowest Mach number case in Fig. 5 exhibits larger errors for the higher frequencies. These errors are a direct result of the slow convergence to a stationary iteration demonstrated above and inspection of these simulations show they have not quite reached stationarity. In addition to this low frequency error the highest Mach number case (0.5) begins to show significant dispersion errors at the highest frequencies. This is the result of phase errors in the computation and can be removed by additional grids as noted later.

A key parameter in unsteady flow solutions is the degree of grid resolution. The

representative parameter is points-per-wavelength (ppw), but since the wavelength in these computations gets consistently shorter as the frequency is increased, we present a grid refinement study in terms of the number of grids along the length of the combustor. The results are shown in Fig. 6 for grids of 20, 40 and 80 points in the longitudinal direction. The 20 grid point results correspond to approximately 40 points per wavelength at the fundamental frequency of the chamber and to correspondingly fewer ppw as the frequency is increased. The comparison of accuracy with frequency clearly shows these trends. Numerical results are compared with the exact solution for each of 32 frequencies over a range similar to that used in Fig. 5 above for the $M = 0.3$ case. For the 20 grid point case, the accuracy of the numerical solution remains good for the first mode, but as the second mode is approached, the errors begin to grow and the predictions become increasingly poorer. In addition, the amplitude of the second mode is considerably under predicted on this coarse grid. For the 40 and 80 grid-point cases, the numerical results remain very similar to each other and show good agreement with the exact solution to the highest frequencies shown. There is noticeable dispersion error at the highest frequencies on all grids, although the finest grid is the best and the coarsest is worst. In all cases, the temporal resolution was 100 points per period. All computations above were run on the finest grid.

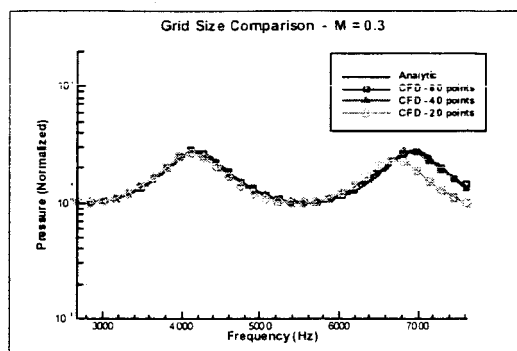


Figure 6. Grid refinement study for longitudinal oscillations and comparison with analytical solution.

The above results are for downstream pressure forcing with mass flow and stagnation temperature fixed at the upstream, inflow boundary. As an assessment of the sensitivity to upstream conditions, we also present in Fig. 7 a set of results for simulations in which the upstream stagnation pressure was held fixed. For this computation, we show only the numerical solutions, and give results for mean flow Mach numbers of 0.1, 0.3 and 0.5. In all cases the response is quantitatively different than when the mass flux was held fixed, but are qualitatively analogous (compare Fig. 7 with Fig. 5). Again the trend is toward lower frequencies for higher Mach numbers, but the trend appears slightly more pronounced. A major difference is that the stagnation pressure boundary condition

produces a significant change in the resonant frequencies and allow damped oscillations at the upstream end.

TRANSVERSE COMBUSTOR SIMULATIONS

The transverse mode computations are for a two-dimensional chamber that simulates a rectangular experimental concept [1]. For this case we use a constant area duct for analytical and computational simulations and chambers with one, two, four and eight nozzles for the simulations. The simulations are for a chamber width of 8" and a length of 3.2". The predictions are for non-uniform upstream mass forcing. Temperature and pressure conditions are similar to those for the longitudinal configuration and result in first and second transverse modes of 3000 and 6000 Hz. The first longitudinal mode is at 7200 Hz. The results are shown in Fig. 8.

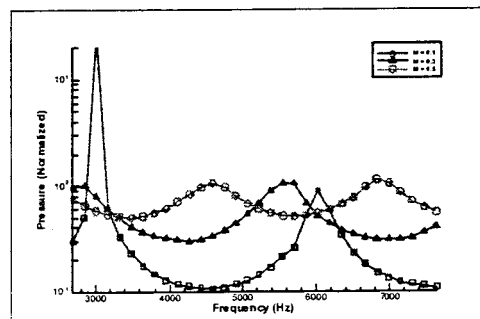


Figure 7. Longitudinal mode response for fixed upstream stagnation pressure. Mean flow Mach numbers, 0.1, 0.3, and 0.5.

The results in Fig. 8 are for two mean flow Mach numbers, $M = 0.1$ and $M = 0.3$ and obtained from numerical simulations. A series of grid resolutions were again computed but are omitted here for brevity. The upstream forcing was done by varying the stagnation pressure in asymmetric fashion to generate transverse disturbances. Response were calculated for a total of 24 modes. The pressure response is reported at the top of the chamber half way between the inlet and exit planes. Again the results show a substantial dependence upon the mean flow Mach number with the higher value producing more nearly uniform response with frequency. mid-point of the chamber results shown are

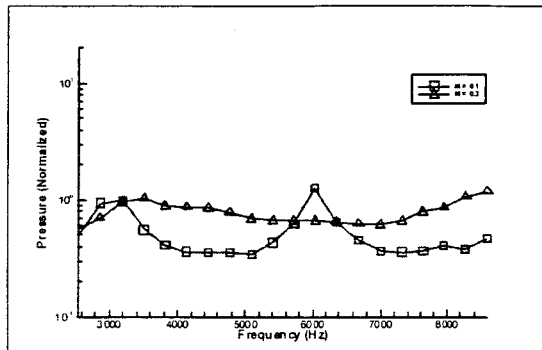


Figure 8. Frequency response for transverse mode chamber. Mean flow Mach numbers 0.1 and 0.3. Numerical simulation

A series of transverse mode calculations have also been computed in the presence of multiple nozzles using upstream forcing. The geometric configurations with a single nozzle and four nozzles are given in Fig. 1 above. An eight-nozzle configuration is given in Fig. 9 below. Time-variations of the flow in these multiple nozzle cases are similar to those for the constant area duct although the presence of the convergence has a minor effect. Mean flow variations in these computations were obtained by varying the nozzle area for choked flow conditions.

Finally we note that a series of computations for the effects of nozzles on the longitudinal chamber has also been computed to ascertain the effects of a finite length nozzle

on the modes and also to assess any possible difference from conventional and 'inverted' nozzles. Geometries for these cases are given in Fig. 2. The inverted nozzles are of interest for experimental investigation of chambers whose length can be varied during a run. The results show that the conventional and inverted nozzles give nearly identical results for the same area ratio.

SUMMARY AND CONCLUSIONS

Computational simulations have been used in conjunction with closed-form analytical solutions to study the acoustic characteristics of laboratory scale combustion chambers. Two geometrical configurations have been addressed, a long chamber that responds to longitudinal modes and a wide, two-dimensional chamber that responds to transverse modes. The longitudinal chamber represents a potential screening mechanism for the relative stability characteristics of candidate injector elements under the supposition that elements susceptible to longitudinal modes will likewise be sensitive to transverse modes. The transverse wave geometry is intended to provide a more direct representation of rocket instabilities and to complement the longitudinal screening and verify its effectiveness.

The closed-form analytical results are used for defining the global topographical characteristics of the instability surfaces and as the first step in verifying the numerical simulations. Without an analytical guide, computational simulations are highly ineffective because hundreds or thousands of simulations are needed to map out the stability characteristics of a given injector/chamber combination. Exact analytical solutions provide precise information on modes shapes, amplitudes and phase relationships that can accurately verify that the

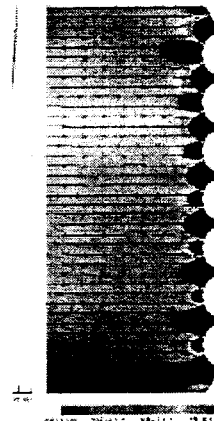


Figure 9. Eight nozzle transverse combustor with pressure oscillations

numerical simulation provides the proper solution to the proposed model. Experimental validation is then needed to evaluate the model itself, not its numerical implementation.

A key issue in uni-element testing is that the mean flow Mach number is generally considerably lower than in the engine, and an initial focus of the present results is to assess how this Mach number scaling affects the stability results. The present results indicate that as the mean Mach number in the chamber is increased, the response to both longitudinal and transverse forcing weakens while the resonant modes decrease in frequency. Large mean flow Mach numbers also lead to broader peaks in response. The results provide a useful means for scaling mean flow Mach number effects in uni-element tests for realistic engine Mach numbers.

The comparisons between analytical and numerical simulations demonstrate that grid resolution that provides from 40 to 80 points per wave can with second-order schemes can produce simulations with errors of less than 1% in amplitude and phase. Numerical simulations for transverse waves in two-dimensional chambers show qualitatively similar results to solutions for the simple constant area geometries used in the analytical results. Estimates of the effect of nozzle length on response are in progress.

ACKNOWLEDGMENTS

This work was accomplished under NASA Space Act Agreement NCC8-200. Our team thanks Brent Harper the COTR, and Garry Lyles and his staff for their technical inputs and encouragement.

REFERENCES

1. Santoro, R. J., Pal, S., Woodward, R. D. and Kalitan D., ***Performance and Stability Characteristics of a Uni-Element Swirl Injector for Oxygen-Rich Stage Combustion Cycles***, 52nd JANNAF Propulsion Meeting, Las Vegas NV, May 10-13, 2004.
2. Miller, K.J., Anderson, W.E., and Heister, S.D., ***Investigation of Liquid Rocket Injector Element Stability Margins***, 52nd JANNAF Propulsion Meeting, Las Vegas NV, May 10-13, 2004.
3. Li, D. Fakhari, K., Sankaran, V. and Merkle, C. L., ***Convergence Assessment of General Fluid Equations on Unstructured Hybrid Grids***, AIAA 2001-2557, June 2001.
4. Li, D. and Merkle, C., ***Analysis of Real Fluid Flows in Converging Diverging Nozzles***, AIAA-2003-4132, 33rd AIAA Fluid Dynamics Conference, Orlando FL, June 23-26, 2003.
5. Merkle, C. L., Sullivan, J. A. Y., Buelow, P. E. O. and Sankaran, V., ***Computation of Flows with Arbitrary Equations of State***, AIAA Journal, Vol. 36, No. 4, pp. 515-521, April 1998.
6. Sankaran, V. and Merkle, C. L., ***Artificial Dissipation Control for Unsteady Computations***, AIAA 2003-3696, 16th AIAA Computational Fluid Dynamics Conference, June 23-26, 2003, Orlando, FL